

Review

Influence of Corrosion-Induced Damage on Mechanical Integrity and Load-Bearing Capability of Cemented Carbides

Yafeng Zheng^{1,2}, Gemma Fargas³ , Elaine Armelin⁴ , Olivier Lavigne⁵ , Qunli Zhang^{1,2} , Jianhua Yao^{1,2} and Luis Llanes^{3,*} 

- ¹ College of Mechanical Engineering, Zhejiang University of Technology, Hangzhou 310023, China
² Institute of Laser Advanced Manufacturing, Zhejiang University of Technology, Hangzhou 310023, China
³ CIEFMA, Department of Materials Science and Engineering, EEBE—Campus Diagonal Besòs, Universitat Politècnica de Catalunya, 08019 Barcelona, Spain
⁴ IMEM, Departament d'Enginyeria Química, EEBE—Campus Diagonal Besòs, Universitat Politècnica de Catalunya, 08019 Barcelona, Spain
⁵ Hyperion Materials and Technologies, 08107 Martorelles, Spain
* Correspondence: luis.miguel.llanes@upc.edu

Abstract: Tungsten carbide based cemented carbides, often simply termed hardmetals, are established forefront materials for tools, structural components, and wear parts with stringent requirements. Several of the technological applications in which they are used include exposure to chemically aggressive media. Under these conditions, failure induced under applied load may be accelerated; and consequently, the service life may be decreased. Within this context, this work addresses the influence of corrosion-induced damage on the mechanical integrity and load-bearing capability of hardmetals at different length scales, i.e., from 100s nanometers to 1000s microns. Experimental data acquired by means of nanoindentation, pyramidal, and spherical indentation, as well as sliding contact (micro- and nanoscratch) techniques, are presented. The attained results allow for identifying guidelines for the microstructural design of these materials under combined consideration of corrosion and mechanical contact as service-like conditions. Discussion of the reported findings includes a critical analysis of corrosion effects on the evolution of microstructure-property-performance interrelations for the materials under consideration.

Keywords: cemented carbides; corrosion; mechanical contact; scratch; mechanical integrity; load-bearing capability; microstructure-property-performance interrelations



Citation: Zheng, Y.; Fargas, G.; Armelin, E.; Lavigne, O.; Zhang, Q.; Yao, J.; Llanes, L. Influence of Corrosion-Induced Damage on Mechanical Integrity and Load-Bearing Capability of Cemented Carbides. *Metals* **2022**, *12*, 2104. <https://doi.org/10.3390/met12122104>

Academic Editor: Walter Lengauer

Received: 29 September 2022

Accepted: 5 December 2022

Published: 7 December 2022

Publisher's Note: MDPI stays neutral with regard to jurisdictional claims in published maps and institutional affiliations.



Copyright: © 2022 by the authors. Licensee MDPI, Basel, Switzerland. This article is an open access article distributed under the terms and conditions of the Creative Commons Attribution (CC BY) license (<https://creativecommons.org/licenses/by/4.0/>).

1. Introduction

The excellent combination of properties exhibited by cemented carbides has made them the preferential choice in a large number of industrial applications demanding high performance under stringent working conditions, e.g., cutting and forming tools, mining bits, and mechanical seals [1]. In addition to exposure to contact loading, wear, or repetitive impacts, some of these applications involve harsh chemical media [1–4]. In this regard and considering the ceramic-metal composite nature of hardmetals, it is now well-established that the metallic binder is preferentially attacked in acid and neutral media, whereas the ceramic phase is the one corroded in alkaline solutions (e.g., Refs. [5–11]). Under these conditions, it has been shown that accelerated failures induced by applied loads may lead to a significant reduction in service life.

Extensive research has been conducted aiming to evaluate either corrosion or tribology response (wear, abrasion, contact loading, or scratch) as separated degradation phenomena in cemented carbides (Figure 1). However, as indicated by a bibliometric analysis done using databases from Scopus or Web of Science, the number of studies addressing the combined action of corrosion and any of the referred tribology-related phenomena in these materials is much more limited. Within this context, existing synergic-like investigations

have been mainly focused on wear–corrosion interaction, following testing methodologies involving either abrasion or sliding contact phenomena [12–22]. Regarding the former, several interesting findings have been documented on the basis of abrasion–corrosion tests conducted in chemically aggressive slurry within a wide range of pH values [13–18]. First, binder dissolution and corresponding removal of tungsten carbide (WC) particles is the rate-controlling step to determine volume loss under strongly acidic conditions (pH = 1.1). Second, WC grains fracture combined with less binder dissolution seems to predominate under weakly acidic conditions (pH = 2.6 and 6.3). Third and finally, overall wear rates are hardly affected in neutral and alkaline conditions. Meanwhile, Gee and co-workers have successfully studied, documented, and analyzed the synergy between corrosion and scratch [19–21]. Among the interesting results reported by them, it must be highlighted that there is an evidenced degradation regarding the microstructural and mechanical integrity of the studied cemented carbides due to the binder leaching.

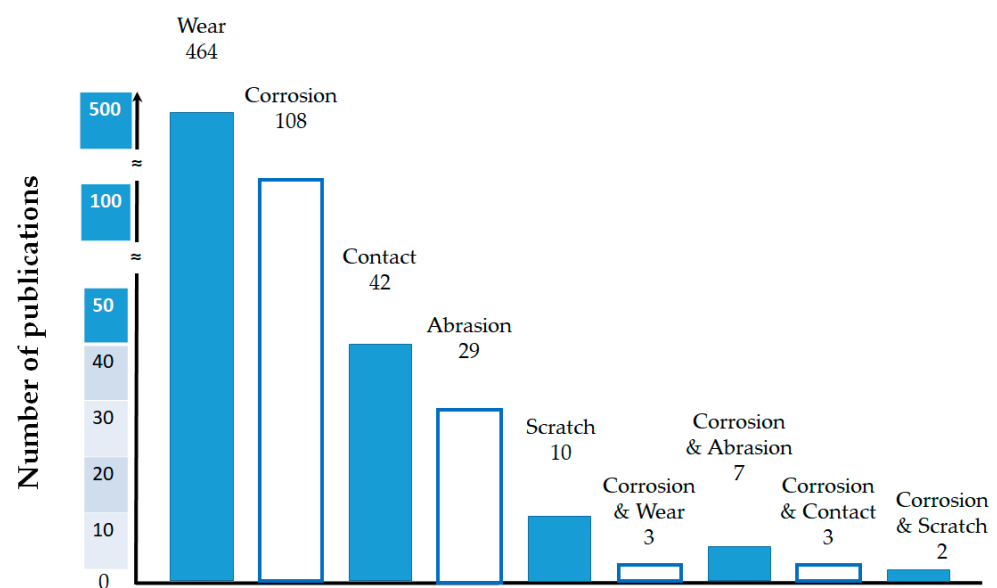


Figure 1. Number of publications reported in open literature addressing either individual or combined action of different degradation phenomena in cemented carbides: corrosion, wear, contact loading, abrasion, and scratch.

The use of small-scale indentation and scratch techniques has been well-established as suitable and valid tool to determine the mechanical and tribological properties of cemented carbides at micro- and nano-metric length scales [23]. The implementation of these testing approaches has allowed for measuring intrinsic hardness and elastic modulus of individual constituent phases [24–29]; assessing the influence of microstructure on sliding contact, scratch, and wear resistance [30–32]; and shedding light on deformation, wear and material removal mechanisms [25–32]. Unfortunately, all the referred works have been conducted on pristine or virgin cemented carbides; hence, there is a significant lack of information about the influence of the damage induced by corrosion on the effective mechanical integrity of hardmetals. Furthermore, testing protocols based on spherical indentation have been successfully used for evaluating the contact response and induced damage in nude and coated cemented carbides [33–42]. In such studies, contact damage was introduced using spheres with curvature radii in the millimeter length scale. However, once again, investigations in most of these works have been exclusively carried out on pristine or virgin cemented carbides. Hence, once again, information addressing the simultaneous action of contact loading (monotonic/cyclic) using spherical indentation and corrosive medium is not only quite scarce but also required.

Following the above ideas, the influence of corrosion on the mechanical response and damage of cemented carbides at different length scales is reviewed on the basis of

recent work published by the authors [43–46]. It includes corrosion-induced changes in the microstructural scenario, small-scale mechanical integrity, load-bearing capability, spherical indentation contact behavior, and corresponding damage scenarios, as summarized in Figure 2.

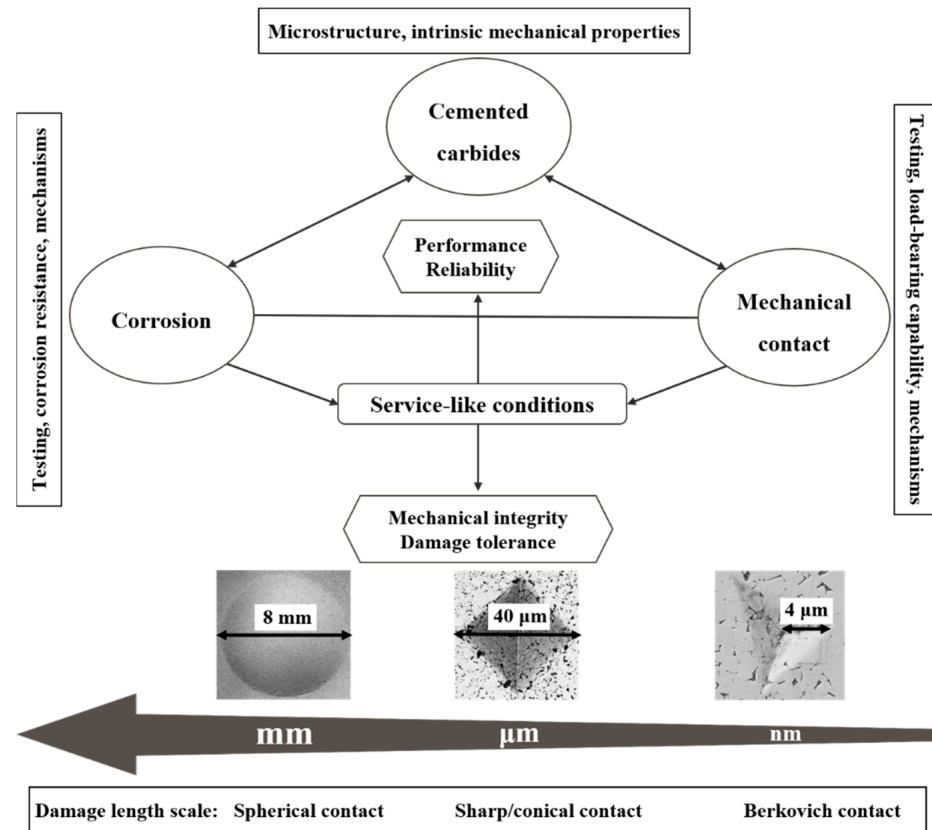


Figure 2. Scheme illustrating the techniques employed and research layout in revised works (Refs. [43–46]).

2. Corrosion-Induced Changes on the Mechanical Integrity of Cemented Carbides

The authors have implemented nanoindentation and nanoscratch tests on a hardmetal consisting of WC particles of about 1.5 μm embedded in a cobalt (Co) based metallic binder (6 wt%), for both pristine and previously corroded conditions. The corresponding surface/subsurface and mechanical integrity changes were then assessed and analyzed at relatively small length scales (100 s to 1000 s nanometers) [43]. The examination of the indented and scratched surface revealed that the small-scale mechanical properties of the studied hardmetal grade (6 CoM) were significantly degraded due to the damage induced by corrosion. In this regard, the non-corroded specimens exhibited a higher indentation and scratch damage resistance response, as concluded from higher hardness and Young's modulus measured (Figure 3a), the narrower and shallower imprints/tracks (Figure 3b,d,e), as well as less spallation and local chipping degree (Figure 3b,e). It could be attributed to the effective deformation compatibility discerned between hard and soft phases, where the intrinsic toughening capability of the metallic binder hampers carbide microfracture; and thus, evades possible pull-out of the grains [31,47]. However, in the case of the corroded condition, a mechanically unsupported carbide skeleton as remnant microstructure was yielded due to the dissolution of the metallic binder (Figure 3c), leading to plastic deformation incompatibility between both phases together with microfracture within contiguous carbide grains. Therefore, a more severe damage scenario is discerned for both indented and scratched surfaces (Figure 3c,f) in terms of larger penetration depth, early fragmentation of WC phases, and easy removal of loose grains.

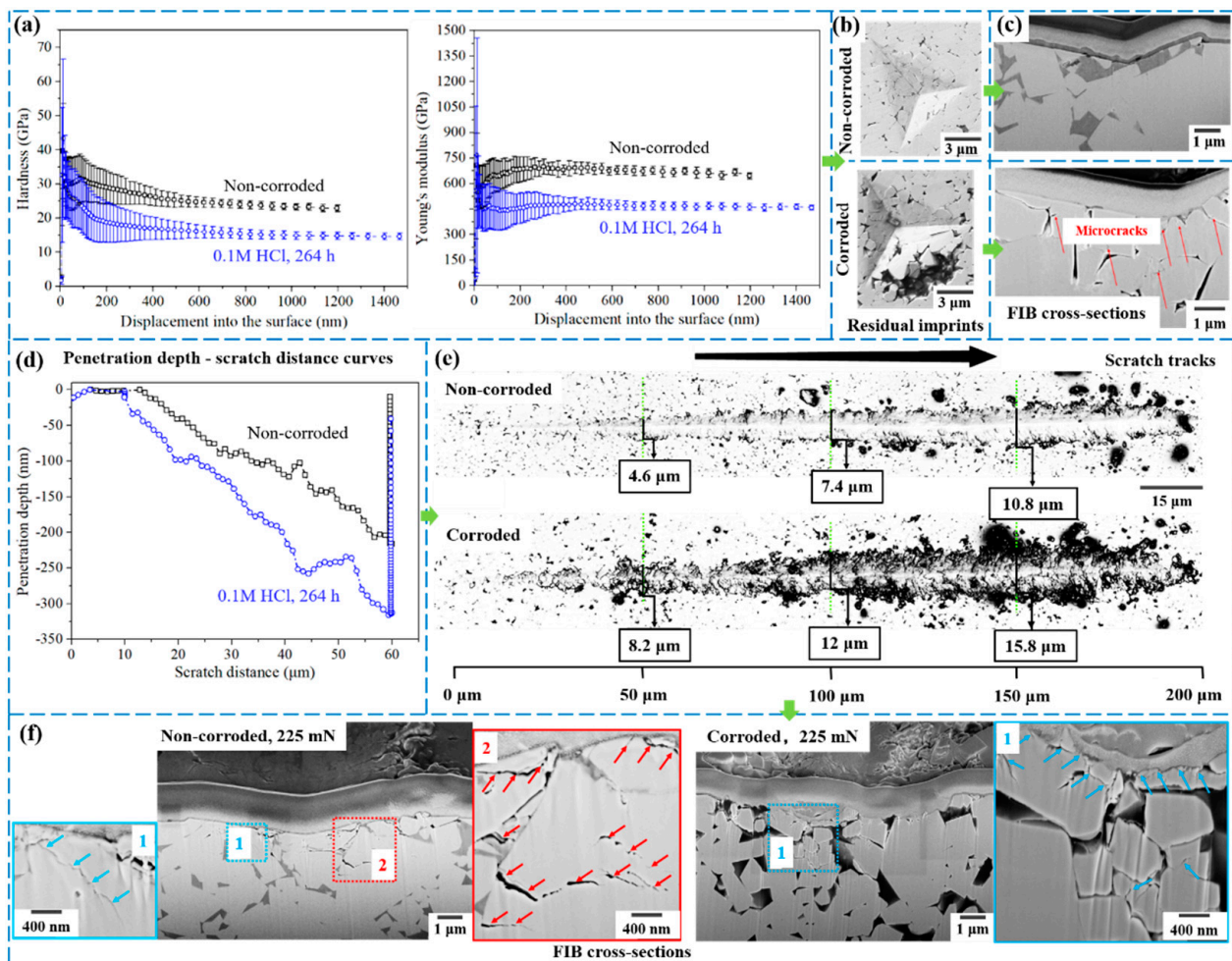


Figure 3. (a) Hardness and Young's modulus values as a function of penetration depth, (b) nanoindentation residual imprints, (c) FIB cross-section of indented surface, (d) typical penetration depth—scratch distance (under increasing applied load condition) curves, (e) micrographs of two scratch tracks, and (f) FIB cross-sections of the scratch track corresponding to a load level of 225 mN for non-corroded and corroded 6CoM samples (adapted from Ref. [43]).

An in-depth understanding of the deformation and damage scenarios may be attained from the inspection of cross-sectional views by means of field emission scanning electron microscopy (FESEM) and focused ion beam (FIB) milling, as shown in Figure 3c,f. Regarding the nanoindentation tests, the collapse of the binderless and porous carbide network at the local level and pronounced multiple cracking was discerned in the corroded condition, while the non-corroded case indicated an effective load-sharing between the soft and hard phases. In the nanoscratch tests, the deformation and fracture features of the virgin specimen were discerned in both phases (Co and WC phases). As the compressive stresses induced by scratching rise, plastic deformation of Co binder first emerges near the interphase boundaries, followed by a series of damage scenarios of extrusion, cracking, and removal of binder phase, microfracture, and subsequent fragmentation of the individual WC grains. Concerning the corroded specimens, strain energy induced by sliding contact is absorbed/released by means of: (1) the removal of loose WC grains near the track edges and (2) the emergence of multiple cracking and internal rupture of individual carbides. It further supported the experimental findings that the effective mechanical integrity of the remaining WC skeleton was markedly lessened, yielding then easy removal of loose grains even by light abrasion.

3. Corrosion Effects on the Load-Bearing Capability and Induced Damage of Cemented Carbides

Exposure to longer corrosion times, together with the use of pyramidal indentation and sliding contact (microscratch), allowed us to extend the study referred to in the previous section to higher length scales, from 10s to 100s of microns in depth [44]. As the area of indentation and scratch-affected zones were significantly increased, a longer corrosion time was chosen for obtaining uniform and rather thick corrosion-affected layers, whose thickness is similar to the corresponding damage depth.

It was found that the load-bearing capability and crack extension resistance of the investigated cemented carbide grade were markedly degraded for longer exposure times to corrosive media. The former is manifested in changes in the damage-related features, such as deeper penetration, larger residual imprints, wider scratch track, as well as decreased hardness value, as the corrosion time increases from 1 day to 11 days. The latter is evidenced in terms of the decreased crack resistance values as a function of corrosion time. In this regard, the lessened resistance against cracking phenomena of cemented carbides is directly linked to the energy absorbed during the constrained plastic stretching of Co binder ligament as cracks extend [48,49]. In this sense, the toughening effect due to ductile ligament reinforcement depends largely on the volume fraction of the binder phase, with the corresponding crack growth (R-curve) resistance increasing as the binder content gets higher [50,51]. Thus, in the authors' investigation, the corrosive exposure results in the effective removal of the ductile metallic phase, implying that the referred toughening is no longer operative, leading to a gradually lowered energy required for subcritical crack propagation as corrosion time increases. Interestingly, the above-mentioned corrosion-induced lessening effects were found to decrease as exposure time increased, and no difference was discerned after 7 days of immersion. In this regard, a relative indentation depth (R) parameter, which is defined by the ratio between indentation depth and layer thickness, may be used to describe the coating thickness effect on measured mechanical properties [44]. Within this context, it has been reported that the measured mechanical properties of a dense coating are not affected by the substrate response as long as R is lower than 0.1, while in the case of a porous film on a hard substrate, such critical R can even reach 0.3 [52,53]. Within the experimental scatter of the results, the calculated R values in the condition of 1 day and 3 days of immersion are about 0.2–0.3, then sustaining the description of the corroded specimens as systems consisting of a porous ceramic layer on top of a very hard composite substrate.

Corrosion effects on damage scenarios induced during indentation and scratch tests may be further understood by analyzing the existing crack-microstructure interaction (Figure 4). For both testing conditions (i.e., pyramidal indentation and micro-scratch), a well-defined cracking system is discerned for the non-corroded conditions, while in the corroded case, multiple branched fissures confined within the porous-like degraded layers are observed. This is in agreement with previous studies on sintered steels containing a relatively large intrinsic porosity, where cracks exhibit pronounced branching, as they are prone to follow easy paths of interconnected pores [54]. Thus, in the corroded case, the subsurface crack propagation behavior is associated with the effectiveness of small-length-scale interactions between cracks and cavities within the binderless WC framework [55]. In this regard, the pores left after the binder is dissolved act as both an assemblage of many stress concentrators and crack precursors [56]. Hence, when a load is applied, main cracks first propagate toward the bulk, and then additional microstructurally short cracks nucleate at the referred pores to subsequently extend steadily outwards.

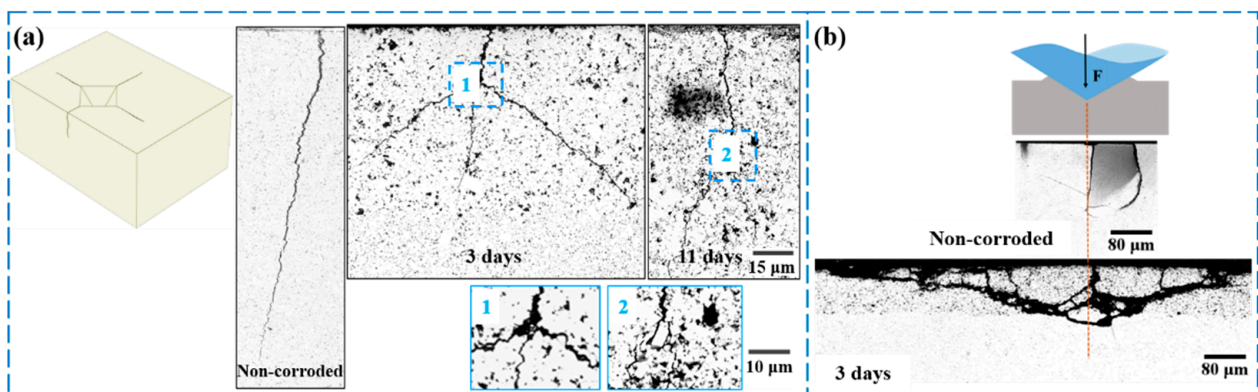


Figure 4. (a) Cross-section view of cracking phenomena resulting from pyramidal indentation under an applied load of 294 N for specimens previously exposed to corrosion media during different times, and (b) subsurface cracking scenario induced by scratching for non-corroded and corroded 6CoM samples (adapted from Ref. [44]).

4. Corrosion-Induced Changes on Hertzian Contact Damage in Cemented Carbides

Spherical indentation is an interesting and feasible technique for the evaluation of corrosion effects on the mechanical integrity of hardmetals at even higher length scales, i.e., up to 1000 microns, closer to those involved under service-like conditions. It was implemented in materials exposed to an acidic media for different times, aiming to document and analyze the changes observed in the indentation stress-strain response [45]. The study was conducted in three microstructurally distinct hardmetal grades, corresponding to modifications of the reference 6CoM one by the addition of chromium (6CoCrM) and/or substitution of cobalt by nickel (6NiCrM) within the chemical nature of the metallic binder. Furthermore, the corresponding surface and subsurface features were assessed by the use of advanced characterization techniques, such as the bonding interface technique combined with FIB/FESEM observation.

Similar to the phenomenon discerned in the former sections, corroded hardmetals show a lower load-bearing capability than pristine ones. This was manifested by the increased depth of the residual imprints at a given load, as well as the deteriorated stress-strain behavior discerned after corrosion. In this regard, the generation of porous/binderless corroded layers directly led to the gradual increase of the indentation depth at a given load as immersion time gets longer [43,44]. On the other hand, indentation strain-stress response shows significant dependence on the depth of the corroded layers. In this sense, quasi-plastic deformation was largely controlled by the uncorroded substrate, which can be attributed to the very low ratio between layer thickness and indenter radius. As the layer thickness increases (from 10 s to 100 s microns), the quasi-plastic deformation tends to be confined within the porous/binderless corroded layers. For the most aggressive corrosion condition (i.e., with the immersion time of 11 days), the measured indentation stress decay is maximum for 6CoM (23%), intermediate for 6NiCrM (20%), and minimum for 6CoCrM (13%).

The detrimental corrosion effect on contact damage was also evidenced, as given by the observation of a lower critical load for the emergence of incipient cracks and more severe damage scenarios at the surface level, as shown in Figure 5. Regarding the non-corroded condition, in agreement with previous studies [33,57,58], contact damage was found to evolve from an initial partial ring crack to full ring ones as the applied load increased. For the corroded condition, besides the similar evolution discerned in the pristine hardmetals, radial cracks (located in the deformed zone and the edge of the plastic zone) and even specimen breakage were evidenced. Once again, this is attributed to the effective removal of the metallic phase, yielding a loose and porous WC skeleton. Hence, toughening mechanism, based on ductile ligament reinforcement, is no longer operative at the surface level of corroded specimens. Within this context, the shear stress during the

unloading process may be recalled for explaining the initiation of radial cracks in the edge of the plastic zone. Similar to the evaluation done on the basis of indentation stress decay, 6CoCrM may be proposed as the best option, as compared to the other two hardmetal grades investigated, considering the critical load for the initiation of cracks and damage scenario as figures of merit for material selection, for the service condition involving the combined action of corrosion and contact loads.

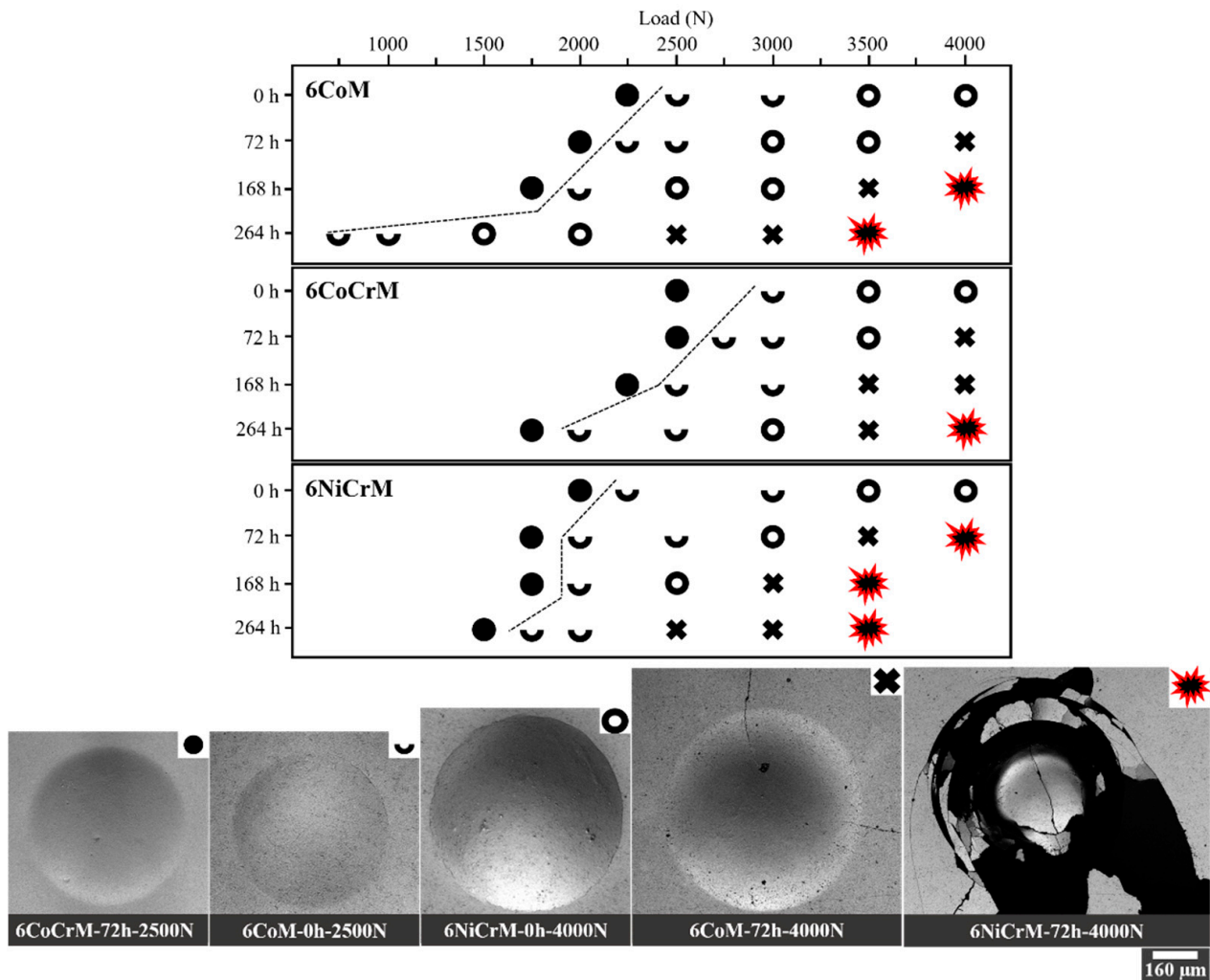


Figure 5. Damage evolution diagram for 6CoM, 6CoCrM, and 6NiCrM samples as a function of indentation load and corrosion time. Main damage features ascribed to each symbol (no cracks, partial ring crack, full ring crack, radial crack, and specimen breakage) are shown within the legend, including images of representative events (adapted from Ref. [45]).

Furthermore, the corresponding surface and subsurface damage mechanisms were analyzed by means of FESEM, as shown in Figure 6. Concerning the uncorroded condition, the contact damage is mainly reflected by cracking, mainly crossing the two-phase microstructure at the surface level and plastically deformed WC grains at both surface and subsurface levels. Regarding the corroded specimens, the surface damage scenario is dominated by well-developed radial cracks accompanied by significant WC grain removal, cracking, and fragmentation of the particles together with micrometric cavities caused by dislodged carbides. At the subsurface level, different damage scenarios were observed in the corroded zone, as compared to those found in the region below the interface between the corroded and uncorroded zone. In the former case, microcracks are distributed throughout the deformed area as a result of the role played by the pores left after the

binder was leached out, i.e., small stress concentrators and crack precursors [45]. Regarding the latter, the strain energy is absorbed by compatible plastic deformation between the constitutive phases.

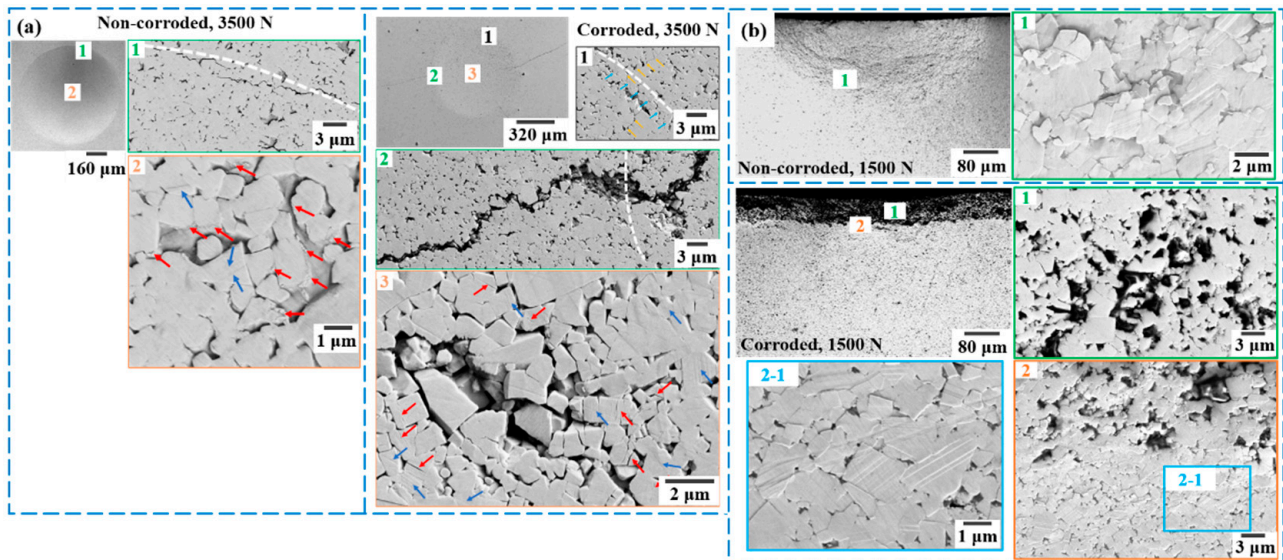


Figure 6. FESEM images of the indented area (residual imprints) for (a) 6NiCrM specimen, and (b) 6NiCrM “clamped-interface” specimens: micrographs of subsurface damage for non-corroded and corroded (7 days) conditions (adapted from Ref. [45]).

5. Corrosion-Induced Changes on Contact Fatigue Response of Cemented Carbides

Hardmetal tools and components are often exposed to working conditions involving both cyclic loading and corrosion. Thus, the effect of corrosion-induced changes on the contact fatigue response and associated damage in the reference 6CoCrM hardmetal grade was further investigated by the authors [46]. It fills the information gaps regarding the use of spherical indentation to evaluate the contact fatigue behavior of cemented carbides, considering the combined action of corrosion and cyclic loading at a length scale of up to 1000 microns. Furthermore, the study evaluated the influence of microstructural changes, previously induced by corrosion, on the damage scenario and corresponding failure micromechanisms resulting from the repetitive contact loading.

Surface damage induced by repetitive contact loads was inspected by means of laser scanning confocal microscopy (LSCM) on both non-corroded and corroded specimens, and the main results are shown in Figure 7. Similar to the behavior reported under monotonic loading, the cyclic contact damage of pristine hardmetal was found to evolve from partial ($N_c = 10 - 10^3$) to (multiple) full ring cracks ($N_c = 10^3 - 10^5$) as the number of cycles increased. Besides, additional information regarding the removal of carbide grains and discrete cohesive chipping at the edge of residual imprints was discerned. Concerning the corroded condition, cracking emergence and evolution took place earlier ($N_c = 10$). Moreover, within the range of the number of cycles studied ($N_c = 10 - 10^5$), changes in the damage scenario were rather ill-defined with gradual transitions. The referred evolution was further inspected for both non-corroded and corroded conditions by means of FESEM, as shown in Figure 8a. It was found that the uniqueness of cracking as an observed damage phenomenon disappears once a relatively high number of cycles is reached (i.e., about 10^5) for the non-corroded condition. Hence, some grain pull-out and oxidation phenomena could be clearly discerned near the crack path. In this regard, similar to the phenomenon reported in previous studies [59–61], the former may be ascribed to frictional-like wear mechanisms. Then, it is speculated that a high enough flash temperature was reached inside the slip region due to shear during relative displacement between contact areas at small length scales, which promotes the oxidation of the binder phase (Figure 8b). In the case of

the corroded condition, ring cracks get less discerned as the number of cycles gets higher, cavities then becoming the only feature near the contour of indentation impression (Figures 7 and 8a). In this regard, the intrinsic toughening of cemented carbides is completely absent after the binder is leached out; thus, the stresses required for dislodging WC grains may be significantly lowered. The energy needed for the grain pulled out may be lower than for the crack initiation and propagation under cyclic loading conditions. Thus, the accumulated degradation will preferentially lead to the generation of cavity-like features. Subsurface inspection of the damaged zone was carried out by means of FIB/FESEM to obtain a complementary viewpoint of the above-described surface damage scenario, as shown in Figure 8c. Regarding the uncorroded specimen, the analysis was focused on the zone where ring cracks were well-developed. It is shown that the failure micromechanism is manifested by the crack extending throughout the two-phase microstructure after repetitive loading contact. Concerning the corroded condition, significant differences were discerned with respect to damage mechanisms found in the pristine one. At the edge of the indentation impression, looser WC particles were discerned, which will be progressively pulled out as the number of cycles get higher.

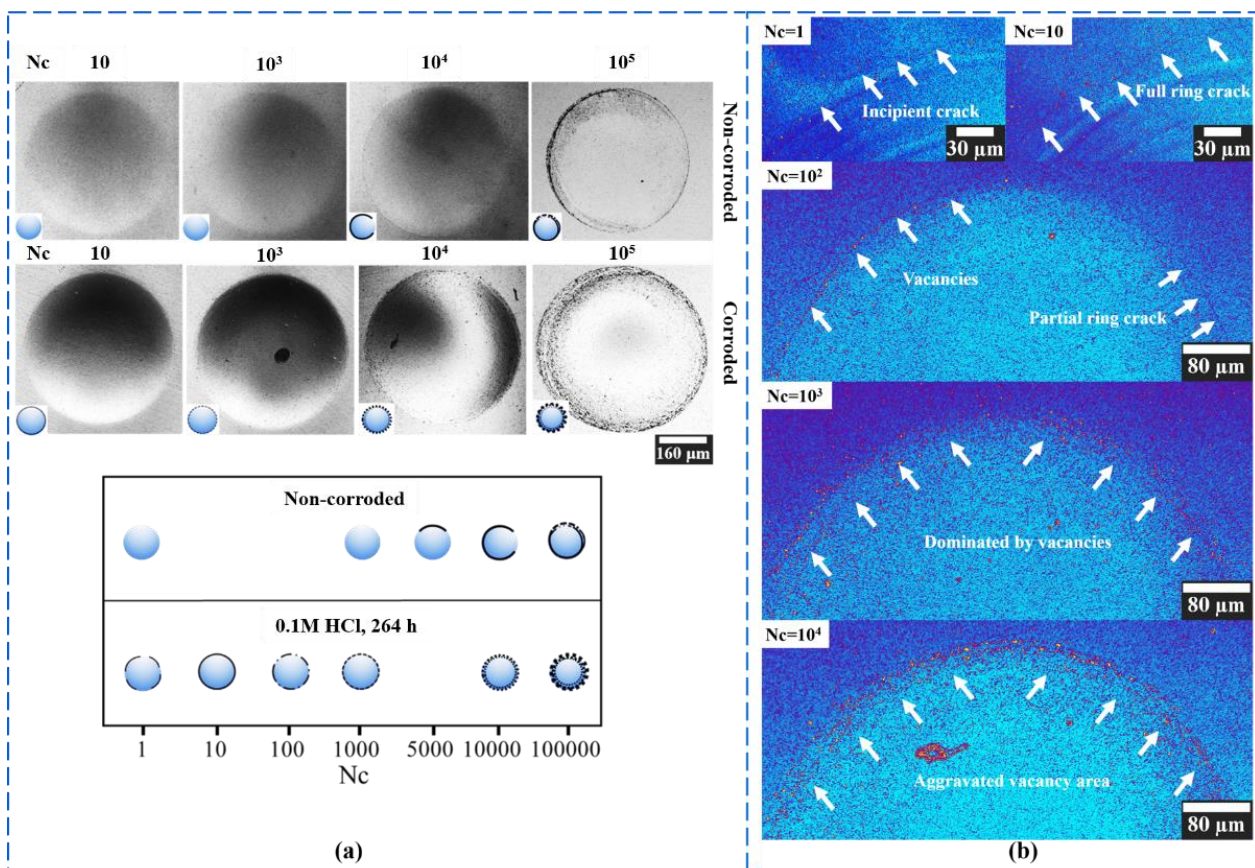


Figure 7. (a) Surface damage scenario and corresponding damage evolution diagrams and (b) LSCM micrographs of damage scenario at regions close to the contour of impressions resulting from contact fatigue tests performed (under a maximum applied load of 2000 N) on corroded specimens at a different number of cycles (adapted from Ref. [46]).

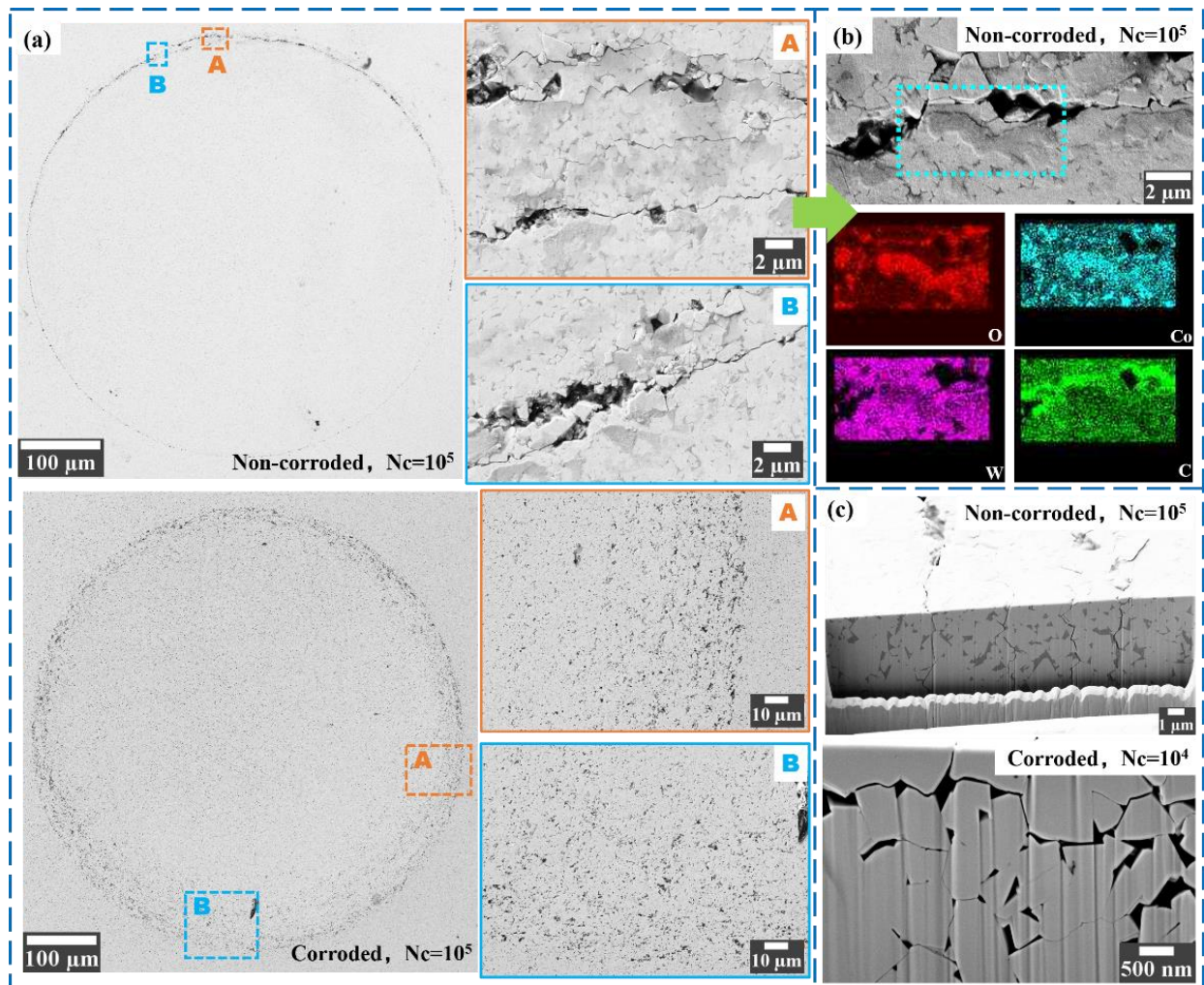


Figure 8. (a) FESEM and LSCM images of indented areas (residual imprints) and enlarged views of corresponding square areas under different experimental conditions, (b) EDX mapping of residual imprint in an uncorroded hardmetal sample, and (c) FIB/FESEM cross-section micrographs of Hertzian contact showing deformation and damage scenarios at the contour of residual impressions (adapted from Ref. [46]).

6. Summary

The main objective of this contribution has been to review recent research work focused on the evaluation of the corrosion-induced changes in the mechanical contact response of hardmetals through a wide range of length scales: from 100 s nanometers to 1000 s microns. In doing so, two baseline aspects have been proposed and validated for defining microstructural design criteria for optimization of the performance of cemented carbides under service-like conditions. First, the synergic consideration of basic mechanical properties (i.e., hardness and toughness) and corrosion resistance by means of analysis and discussion of the combined interaction among them through concepts like damage tolerance. Second, the effective use of a wide spectrum of testing techniques: sharp and spherical indentation together with scratch at macro-, micro-, and nano-metric levels. As a final outcome, in-depth knowledge has been gained about the relevant influence of corrosion-induced damage on mechanical properties, load-bearing capability, resistance to crack extension, spherical indentation stress-strain response, Hertzian contact fatigue behavior and corresponding damage scenarios of cemented carbides with distinct microstructures. Furthermore, the study included the assessment of the evolution of microstructure-property-performance interrelations due to the degradation of the material under severe working conditions.

Author Contributions: Conceptualization, L.L., G.F., O.L., E.A. and Y.Z.; methodology, L.L., G.F., E.A. and Y.Z.; software, L.L. and J.Y.; validation, L.L., G.F., E.A. and Y.Z.; formal analysis, Y.Z., L.L., G.F., E.A. and O.L.; investigation, Y.Z.; resources, L.L. and O.L.; data curation, Y.Z.; writing—original draft preparation, Y.Z. and L.L.; writing—review and editing, Y.Z. and L.L.; visualization, Y.Z. and L.L.; supervision, L.L. and G.F.; project administration, L.L. and Q.Z.; funding acquisition, L.L., Q.Z. and J.Y. All authors have read and agreed to the published version of the manuscript.

Funding: This work was financially supported by the collaborative Industry-University program between Hyperion Materials & Technologies and Universitat Politècnica de Catalunya, the Key Project of the National Natural Science Foundation of China (No. 52035014), “Pioneer” and “Leading Goose” Research and Development Program of Zhejiang Province (No. 2022C01117), and partly funded by the Spanish Government (Ministerio de Ciencia e Innovación and Agencia Estatal de Investigación) and European Union (FEDER) through the project PID2019-106631GB-C41 (AEI/10.13039/501100011033).

Institutional Review Board Statement: Not applicable.

Informed Consent Statement: Not applicable.

Data Availability Statement: Not applicable.

Acknowledgments: Yafeng Zheng acknowledges the Ph.D. scholarship received from China Scholarship Council (No. 201706890018, Beijing, China).

Conflicts of Interest: The authors declare no conflict of interest.

References

1. Pugsley, V.A.; Korn, G.; Luyckx, S.; Sockel, H.G.; Heinrich, W.; Wolf, M.; Feld, H.; Schulte, R. The influence of a corrosive wood-cutting environment on the mechanical properties of hardmetal tools. *Int. J. Refract. Met. Hard Mater.* **2001**, *19*, 311–318. [[CrossRef](#)]
2. Beste, U.; Hartzell, T.; Engqvist, H.; Axén, N. Surface damage on cemented carbide rock-drill buttons. *Wear* **2001**, *249*, 324–329. [[CrossRef](#)]
3. Lu, R.; Minarro, L.; Su, Y.Y.; Shemanski, R.M. Failure mechanism of cemented tungsten carbide dies in wet drawing process of steel cord filament. *Int. J. Refract. Met. Hard Mater.* **2008**, *26*, 589–600. [[CrossRef](#)]
4. Bozzini, B.; Busson, B.; De Gaudenzi, G.P.; Humbert, C.; Mele, C.; Tedeschi, S.; Tadjeddine, A. Corrosion of cemented carbide grades in petrochemical slurries. Part I—Electrochemical adsorption of CN^- , SCN^- and MBT: A study based on in situ SFG. *Int. J. Refract. Met. Hard Mater.* **2016**, *60*, 37–51. [[CrossRef](#)]
5. Human, A.M.; Exner, H.E. The relationship between electrochemical behaviour and in-service corrosion of WC based cemented carbides. *Int. J. Refract. Met. Hard Mater.* **1997**, *15*, 65–71. [[CrossRef](#)]
6. Bozzini, B.; De Gaudenzi, G.P.; Serra, M.; Fanigliulo, A.; Bogani, F. Corrosion behaviour of WC-Co based hardmetal in neutral chloride and acid sulphate media. *Mater. Corros.* **2002**, *53*, 328–334. [[CrossRef](#)]
7. Kellner, F.J.J.; Hildebrand, H.; Virtanen, S. Effect of WC grain size on the corrosion behaviour of WC-Co based hardmetals in alkaline solutions. *Int. J. Refract. Met. Hard Mater.* **2009**, *27*, 806–812. [[CrossRef](#)]
8. Alar, Ž.; Alar, V.; Fabijanić, T.A. Electrochemical corrosion behavior of near-nano and nanostructured WC-Co cemented carbides. *Metals* **2017**, *7*, 69. [[CrossRef](#)]
9. Zheng, Y.; Fargas, G.; Armelin, E.; Lavigne, O.; Llanes, L. Corrosion-induced damage and residual strength of WC-Co, Ni cemented carbides: Influence of microstructure and corrosion medium. *Metals* **2019**, *9*, 1018. [[CrossRef](#)]
10. Fabijanić, T.A.; Kurtela, M.; Škrinjarić, I.; Pötschke, J.; Mayer, M. Electrochemical corrosion resistance of Ni and Co bonded near-nano and nanostructured cemented carbides. *Metals* **2020**, *10*, 224. [[CrossRef](#)]
11. De Gaudenzi, G.P.; Tavola, F.; Tedeschi, S.; Bozzini, B. Corrosion behaviour of cemented carbides with Co- and Ni-alloy binders in the presence of abrasion. *Metals* **2022**, *12*, 1914. [[CrossRef](#)]
12. ASTM G65-00; Standard Test Method for Measuring Abrasion Using the Dry Sand/Rubber Wheel Apparatus. American Society for Testing and Materials: West Conshohocken, PA, USA, 2000.
13. Shipway, P.H.; Wirojanupatump, S. The role of lubrication and corrosion in abrasion of materials in aqueous environments. *Tribol. Int.* **2002**, *35*, 661–667. [[CrossRef](#)]
14. Gant, A.J.; Gee, M.G.; May, A.T. The evaluation of tribo-corrosion synergy for WC-Co hardmetals in low stress abrasion. *Wear* **2004**, *256*, 500–516. [[CrossRef](#)]
15. Gant, A.J.; Gee, M.G.; May, A.T. Microabrasion of WC-Co hardmetals in corrosive media. *Wear* **2004**, *256*, 954–962. [[CrossRef](#)]
16. Shipway, P.H.; Howell, L. Microscale abrasion—Corrosion behaviour of WC-Co hardmetals and HVOF sprayed coatings. *Wear* **2005**, *258*, 303–312. [[CrossRef](#)]
17. Thakare, M.R.; Wharton, J.A.; Wood, R.J.K.; Menger, C. Exposure effects of alkaline drilling fluid on the microscale abrasion–corrosion of WC-based hardmetals. *Wear* **2007**, *263*, 125–136. [[CrossRef](#)]

18. Thakare, M.R.; Wharton, J.A.; Wood, R.J.K.; Menger, C. Investigation of micro-scale abrasion-corrosion of WC-based sintered hardmetal and sprayed coating using in situ electrochemical current-noise measurements. *Wear* **2009**, *267*, 1967–1977. [[CrossRef](#)]
19. Gee, M.G. Model scratch corrosion studies for WC/Co hardmetals. *Wear* **2010**, *268*, 1170–1177. [[CrossRef](#)]
20. Gee, M.G.; Nimishakavi, L. Model single point abrasion experiments on WC/Co hardmetals. *Int. J. Refract. Met. Hard Mater.* **2011**, *29*, 1–9. [[CrossRef](#)]
21. Gant, A.J.; Gee, M.G.; Gohil, D.D.; Jones, H.G.; Orkney, L.P. Use of FIB/SEM to assess the tribo-corrosion of WC/Co hardmetals in model single point abrasion experiments. *Tribol. Int.* **2013**, *68*, 56–66. [[CrossRef](#)]
22. Gee, M.G.; Mingard, K.P.; Gant, A.J.; Jones, H.G. FIB/SEM determination of sub-surface damage caused by micro-tribology scratching of WC/Co hardmetal samples. In Proceedings of the 1st International Conference on 3D Materials Science, Seven Springs, PA, USA, 8–12 July 2012; De Graef, M., Poulsen, H.F., Lewis, A., Simmons, J., Spanos, G., Eds.; Wiley: Hoboken, NJ, USA, 2016; pp. 25–30.
23. Naughton-Duszová, A.; Csanádi, T.; Sedlák, R.; Hvizdoš, P.; Dusza, J. Small-scale mechanical testing of cemented carbides from the micro- to the nano-level: A review. *Metals* **2019**, *9*, 502. [[CrossRef](#)]
24. Gee, M.G.; Roebuck, B.; Lindahl, P.; Andren, H.-O. Constituent phase nanoindentation of WC/Co and Ti(C,N) hard metals. *Mater. Sci. Eng. A* **2002**, *209*, 128–136. [[CrossRef](#)]
25. Duszová, A.; Halgaš, R.; Břanda, M.; Hvizdoš, P.; Lofaj, F.; Dusza, J.; Morgiel, J. Nanoindentation of WC-Co hardmetals. *J. Eur. Ceram. Soc.* **2013**, *33*, 2227–2232. [[CrossRef](#)]
26. Roa, J.J.; Jiménez-Piqué, E.; Verge, C.; Tarragó, J.M.; Mateo, A.; Fair, J.; Llanes, L. Intrinsic hardness of constitutive phases in WC-Co composites: Nanoindentation testing, statistical analysis, WC crystal orientation effects and flow stress for the constrained metallic binder. *J. Eur. Ceram. Soc.* **2015**, *35*, 3419–3425. [[CrossRef](#)]
27. Roa, J.J.; Sudharshan Phani, P.; Oliver, W.C.; Llanes, L. Mapping of mechanical properties at microstructural length scale in WC-Co cemented carbides: Assessment of hardness and elastic modulus by means of high speed massive nanoindentation and statistical analysis. *Int. J. Refract. Met. Hard Mater.* **2018**, *75*, 211–217. [[CrossRef](#)]
28. Sandoval, D.A.; Roa, J.J.; Ther, O.; Tarrés, E.; Llanes, L. Micromechanical properties of WC-(W,Ti,Ta,Nb)C-Co composites. *J. Alloys Compd.* **2019**, *777*, 593–601. [[CrossRef](#)]
29. Besharatloo, H.; de Nicolás, M.; Roa, J.J.; Dios, M.; Mateo, A.; Ferrari, B.; Gordo, E.; Llanes, L. Assessment of mechanical properties at microstructural length scale of Ti(C,N)–FeNi ceramic-metal composites by means of massive nanoindentation and statistical analysis. *Ceram. Int.* **2019**, *45*, 20202–20210. [[CrossRef](#)]
30. Ndlovu, S.; Durst, K.; Göken, M. Investigation of the sliding contact properties of WC-Co hard metals using nanoscratch testing. *Wear* **2007**, *263*, 1602–1609. [[CrossRef](#)]
31. Sun, H.Q.; Irwan, R.; Huang, H.; Stachowiak, G.W. Surface characteristics and removal mechanism of cemented tungsten carbides in nanoscratching. *Wear* **2010**, *268*, 1400–1408. [[CrossRef](#)]
32. Csanádi, T.; Novák, M.; Naughton-Duszová, A.; Dusza, J. Anisotropic nanoscratch resistance of WC grains in WC-Co composite. *Int. J. Refract. Met. Hard Mater.* **2015**, *51*, 188–191. [[CrossRef](#)]
33. Tarrés, E.; Torres, Y.; Anglada, M.; Llanes, L. Daño por contacto hertziano en carburos cementados WC-Co: Influencia de la microestructura y de los parámetros de contacto. *Anales Mecánica de la Fractura* **2005**, *22*, 300–305.
34. Tarrés, E.; Ramírez, G.; Gaillard, Y.; Jiménez-Piqué, E.; Llanes, L. Contact fatigue behavior of PVD-coated hardmetals. *Int. J. Refract. Met. Hard Mater.* **2009**, *27*, 323–331. [[CrossRef](#)]
35. Llanes, L.; Tarrés, E.; Ramírez, G.; Botero, C.A.; Jiménez-Piqué, E. Fatigue susceptibility under contact loading of hardmetals coated with ceramic films. *Procedia Eng.* **2010**, *2*, 299–308. [[CrossRef](#)]
36. Zhang, H.B.; Lu, Q.; Zhang, L.; Fang, Z.Z. Dependence of microcrack number density on microstructural parameters during plastic deformation of WC-Co composite. *Int. J. Refract. Met. Hard Mater.* **2010**, *28*, 434–440. [[CrossRef](#)]
37. Góez, A.; Coureaux, D.; Ingebrand, A.; Reig, B.; Tarrés, E.; Mestra, A.; Mateo, A.; Jiménez-Piqué, E.; Llanes, L. Contact damage and residual strength in hardmetals. *Int. J. Refract. Met. Hard Mater.* **2012**, *30*, 121–127. [[CrossRef](#)]
38. Yang, J.; García Marro, F.; Trifonov, T.; Odén, M.; Johansson-Jøesaar, M.P.; Llanes, L. Contact damage resistance of TiN-coated hardmetals: Beneficial effects associated with substrate grinding. *Surf. Coat. Tech.* **2015**, *275*, 133–141. [[CrossRef](#)]
39. El Azhari, I.; García, J.; Soldera, F.; Suarez, S.; Jiménez-Piqué, E.; Mücklich, F.; Llanes, L. Contact damage investigation of CVD carbonitride hard coatings deposited on cemented carbides. *Int. J. Refract. Met. Hard Mater.* **2020**, *86*, 105050. [[CrossRef](#)]
40. Roa, J.J.; Simison, S.; Grasso, J.; Arcidiacono, M.; Escalada, L.; Soldera, F.; García, J.; Sosa, A.D. Cyclic contact fatigue of cemented carbides under dry and wet conditions: Correlation between microstructure, damage and electrochemical behavior. *Int. J. Refract. Met. Hard Mater.* **2020**, *92*, 105279. [[CrossRef](#)]
41. Sosa, A.D.; Collado-Ciprés, V.; García, J.L.; Dalibón, E.L.; Escalada, L.; Roa, J.J.; Soldera, F.; Brühl, S.P.; Llanes, L.; Simison, S. Contact fatigue behavior of α -Al₂O₃-Ti(C,N) CVD coated WC-Co under dry and wet conditions. *Mater. Lett.* **2021**, *284*, 129012. [[CrossRef](#)]
42. Collado-Ciprés, V.; Dalibón, E.L.; García, J.; Escalada, L.; Roa, J.J.; Jiménez-Piqué, E.; Soldera, F.; Brühl, S.P.; Simison, S.; Llanes, L.; et al. Contact fatigue behaviour of CVD coated cemented carbides in dry and wet conditions. *Wear* **2022**, *492–493*, 204215. [[CrossRef](#)]

43. Zheng, Y.F.; Fargas, G.; Besharatloo, H.; Serra, M.; Roa, J.J.; Armelin, E.; Lavigne, O.; Llanes, L. Assessment of corrosion-induced changes on the mechanical integrity of cemented carbides at small length scales. *Int. J. Refract. Met. Hard Mater.* **2019**, *84*, 105033. [[CrossRef](#)]
44. Zheng, Y.F.; Fargas, G.; Lavigne, O.; Llanes, L. Indentation and scratch testing of medium-grained WC-6%wtCo: Corrosion effects on load-bearing capability and induced damage. *Ceram. Int.* **2020**, *46*, 17591–17598. [[CrossRef](#)]
45. Zheng, Y.F.; Fargas, G.; Lavigne, O.; Roitero, E.; Llanes, L. Corrosion-induced changes on Hertzian contact damage in cemented carbides. *Int. J. Refract. Met. Hard Mater.* **2020**, *92*, 105334. [[CrossRef](#)]
46. Zheng, Y.F.; Fargas, G.; Lavigne, O.; Serra, M.; Coureaux, D.; Zhang, P.P.; Yao, Z.H.; Zhang, Q.L.; Yao, J.H.; Llanes, L. Contact fatigue of WC-6%wtCo cemented carbides: Influence of corrosion-induced changes on emergence and evolution of damage. *Ceram. Int.* **2022**, *48*, 5766–5774. [[CrossRef](#)]
47. Zuñega, J.C.P.; Gee, M.G.; Wood, R.J.K.; Walker, J. Scratch testing of WC/Co hardmetals. *Tribol. Int.* **2012**, *54*, 77–86. [[CrossRef](#)]
48. Sigl, L.S.; Exner, H.E. Experimental study of the mechanics of fracture in WC–Co alloys. *Metall. Mat. Trans. A* **1987**, *18*, 1299–1308. [[CrossRef](#)]
49. Tarragó, J.M.; Jiménez-Piqué, E.; Schneider, L.; Casellas, D.; Torres, Y.; Llanes, L. FIB/FESEM experimental and analytical assessment of R-curve behavior of WC-Co cemented carbides. *Mater. Sci. Eng. A* **2015**, *645*, 142–149. [[CrossRef](#)]
50. Raddatz, O.; Schneider, G.A.; Claussen, N. Modelling of R-curve behavior in ceramic/metal composites. *Acta Mater.* **1998**, *46*, 6381–6395. [[CrossRef](#)]
51. Tarragó, J.M.; Coureaux, D.; Torres, Y.; Casellas, D.; Al-Dawery, I.; Schneider, L.; Llanes, L. Microstructural effects on the R-curve behavior of WC-Co cemented carbides. *Mater. Design* **2016**, *97*, 492–501. [[CrossRef](#)]
52. Cai, X.; Bangert, H. Hardness measurements of thin films-determining the critical ratio of depth to thickness using FEM. *Thin Solid Films* **1995**, *265*, 59–71. [[CrossRef](#)]
53. Gamonpilas, C.; Esteban, P.B. On the effect of substrate properties on the indentation behavior of coated systems. *Mater. Sci. Eng. A* **2004**, *380*, 52–61. [[CrossRef](#)]
54. Carabajar, S.; Verdu, C.; Hamel, A.; Fougères, R. Fatigue behavior of a nickel alloyed sintered steel. *Mater. Sci. Eng. A* **1998**, *257*, 225–234. [[CrossRef](#)]
55. Rice, R.W. The porosity dependence of physical properties of materials: A summary review. *Key Eng. Mater.* **1996**, *115*, 1–20. [[CrossRef](#)]
56. Holmes, J.; Queeney, R.A. Fatigue crack initiation in a porous steel. *Powder Metall.* **1985**, *28*, 231–235. [[CrossRef](#)]
57. Zhang, H.B.; Fang, Z.Z.; Belnap, J.D. Quasi-plastic deformation of WC-Co composites loaded with a spherical indenter. *Metall. Mater. Trans. A* **2007**, *38*, 552–561. [[CrossRef](#)]
58. Zhang, H.B.; Fang, Z.Z. Characterization of quasi-plastic deformation of WC-Co composite using Hertzian indentation technique. *Int. J. Refract. Met. Hard Mater.* **2008**, *26*, 106–114. [[CrossRef](#)]
59. Lathabai, S.; Rödel, J.; Lawn, B.R. Cyclic fatigue from frictional degradation at bridging grains in alumina. *J. Am. Ceram. Soc.* **1991**, *74*, 1340–1348. [[CrossRef](#)]
60. Dauskardt, R.H. A frictional-wear mechanism for fatigue-crack growth in grain bridging ceramics. *Acta Metall. Mater.* **1993**, *41*, 2765–2781. [[CrossRef](#)]
61. Gilbert, C.J.; Dauskardt, R.H.; Ritchie, R.O. Behavior of cyclic fatigue cracks in monolithic silicon nitride. *J. Am. Ceram. Soc.* **1995**, *78*, 2291–2300. [[CrossRef](#)]